

Infinites of stable periodic orbits in systems of coupled oscillators

Peter Ashwin*

School of Mathematical Sciences, Laver Building, University of Exeter, Exeter EX4 4QE, United Kingdom

Alastair M. Rucklidge† and Rob Sturman‡

Department of Applied Mathematics, University of Leeds, Leeds LS2 9JT, United Kingdom

(Received 14 January 2002; published 3 September 2002)

We consider the dynamical behavior of coupled oscillators with robust heteroclinic cycles between saddles that may be periodic or chaotic. We differentiate attracting cycles into types that we call *phase resetting* and *free running* depending on whether the cycle approaches a given saddle along one or many trajectories. At loss of stability of attracting cycling, we show in a phase-resetting example the existence of an infinite family of stable periodic orbits that accumulate on the cycling, whereas for a free-running example loss of stability of the cycling gives rise to a single quasiperiodic or chaotic attractor.

DOI: 10.1103/PhysRevE.66.035201

PACS number(s): 05.45.Ac, 05.45.Xt, 47.52.+j

Physical systems where an invariant subspace, or set of subspaces, are preserved because of symmetry or other constraint give rise to a number of new types of robust behavior (i.e., behavior that is robust to perturbations that preserve the structure) that would be highly degenerate for systems without the symmetry or constraint. There is an extensive literature discussing theory and examples of this for a variety of physical problems [1].

Structurally stable heteroclinic cycles between equilibria are well documented in ordinary differential equations with symmetries. Examples have been found in many applications such as rotating convection and population dynamics [2], where the system repeatedly spends long periods of time near one equilibrium state, then rapidly switches to another. Heteroclinic cycles between chaotic saddles are also robust in systems with symmetry; these have been found in coupled oscillators [3] and models of planar magnetoconvection [4], the latter example being a cycle alternating between equilibria and chaotic saddles. This kind of behavior arises in many symmetric physical systems of sufficient complexity. In coupled oscillator examples, initially one oscillator is active (it could be periodic or chaotic) while the others are suppressed; later, one of these becomes active and quenches the original active oscillator, and so on. This phenomenon is the counterpart of synchronization.

By analogy with cycles between equilibria for flows, whether such cycling between periodic orbits or chaotic saddles is an attractor or not can be determined by examining the ratios of Lyapunov exponents at the saddles [4,5]. The cycling loses stability at a bifurcation which occurs when rates of linear expansion and contraction become equal (a *resonance* of Lyapunov exponents). Numerical simulations in Ref. [4] suggest that such a resonance creates a large number of periodic attractors that branch from the cycling chaos. By contrast, for the skew-product example of cycling chaos examined in Ref. [5] the resonance was found to give

rise not to periodic orbits but to a chaotic attractor with average cycling chaos, or to quasiperiodicity that is intermittent (stuck on) to the cycling chaos.

In this note, we aim to reconcile these differences by characterizing them as examples of qualitatively different types of cycling. For what we call “phase-resetting” cycling, there is only one approach trajectory towards each saddle within the cycle, while in “free-running” cycling, there are multiple approaches to a single saddle.

We consider two systems of coupled iterated maps where the attraction of the cycling is determined by the strength of the coupling. These maps can be related to flows in the usual way via a Poincaré return map, noting that equilibria and periodic points for a map both correspond to periodic orbits for a flow.

At the resonance bifurcation, for the phase-resetting case we find a plethora of stable high-period periodic orbits with an infinite number of stable periodic orbits accumulating at resonance. For the free-running case the branching attractors are typically unique and quasiperiodic or chaotic. We observe no other scenarios for these models but believe there will be other scenarios for problems with higher dimensional saddles and connections.

Model I is a map of $[0,1]^3$ with \mathbb{Z}_3 symmetry given by

$$(x_{n+1}, y_{n+1}, z_{n+1}) = F_I(x_n, y_n, z_n),$$

where

$$F_I(x, y, z) = (f(x)e^{-\gamma z}, f(y)e^{-\gamma x}, f(z)e^{-\gamma y}),$$

and $f(x) = rx(1-x)$ denotes the logistic map with parameter r . This map clearly preserves the coordinate planes $xyz = 0$. In each variable three distinct types of evolutions are possible. For example, consider x : if $z \ll 1$ and $x \ll 1$ then x grows approximately linearly—the growing phase. For $z \ll 1$ and $x \approx O(1)$, x evolves according to logistic map dynamics—the active phase. Finally if $z \approx O(1)$ the dynamics in the x direction is suppressed by the coupling term—the decaying phase.

*Email address: P.Ashwin@ex.ac.uk

†Email address: A.M.Rucklidge@leeds.ac.uk

‡Email address: rsturman@amsta.leeds.ac.uk

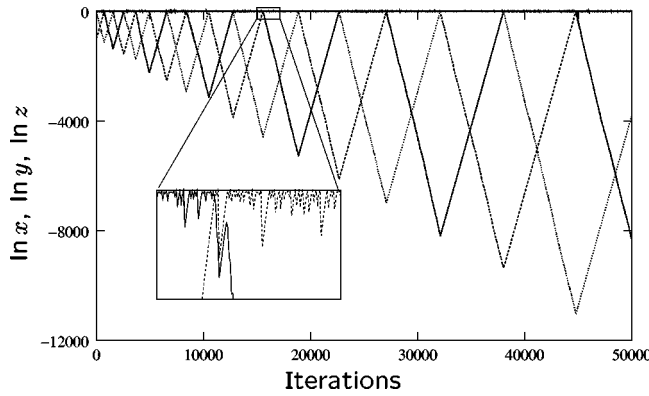


FIG. 1. Attracting cycling chaos, with $r=4.0$, $\gamma=6.0$. Model I is iterated and x, y, z plotted (in logarithmic coordinates) against time. The chaotic behavior is $O(1)$ and is visible in the inset. The trajectory cycles through growing, active, and then decaying phases for each variable, with the length of phase increasing approximately geometrically. The same behavior is found for Model II.

Model II is identical to Model I except that the logistic map f during a *growing phase* is replaced by \tilde{f} ,

$$\tilde{f}(x_n) = \begin{cases} f(x_n), & x_n < \epsilon \text{ or } x_n > f(\epsilon) \\ f^2(\epsilon) = \eta, & x_n \in [\epsilon, f(\epsilon)]. \end{cases}$$

Each time a growing variable reaches the interval $[\epsilon, f(\epsilon)]$ (we use $\epsilon = 10^{-6}$), it is set to $\eta = f^2(\epsilon)$. From this point on, all trajectories then evolve in an identical way. The interval $[\epsilon, f(\epsilon)]$ is of sufficient size to ensure that all trajectories visiting $x_n < \epsilon$ in the growing phase are reset in this way. The effect of the resetting is to force trajectories leaving one saddle to approach the next one close to a single trajectory. This is observed in cycling that alternates between equilibria and chaos for flows [4]. To ensure that $\epsilon < f(\epsilon)$ we take $r \in [1/(1-\epsilon), 4]$.

For both models the coupling is trivial when $\gamma=0$. When the coupling parameter γ is sufficiently strong both the models exhibit robust cycling between invariant sets. In this state, each variable alternates cyclically between the *growing*, the *active*, and the *decaying* phases. We term a change in the phases a “switch.” More precisely, we say a switch occurs when the growing variable exceeds $\ln r/\gamma$. Figure 1 shows a time series for Model I of the three variables cycling, illustrating the three possible phases and the switches between them. As in Ref. [4], for both the models, the number of iterations between switches increases geometrically as trajectories approach the invariant subspaces, and this rate of increase depends on the coupling γ . The rate of increase of switching times approaches zero as γ approaches some critical value from above, which forms the limit of the stability of cycling chaos. Referring to Fig. 1, decreasing γ would result in a slower rate of increase in the number of iterations between switches, and the line formed by connecting the local minima would become more horizontal.

The behavior in the active phase is governed by r . For $r < 3$ the cycles are between period one points; as r is increased (after period doubling) we obtain cycles progres-

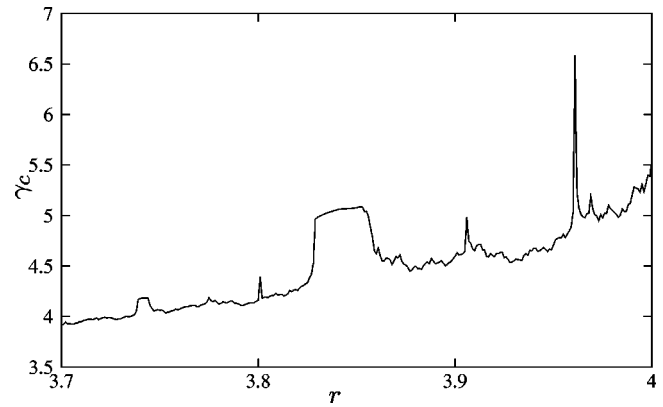


FIG. 2. The critical value of γ at which loss of stability of cycling chaos occurs for Models I and II. Above the line, the cycling is an attractor; below the line the cycling persists but is no longer an attractor.

sively between periodic orbits and then chaotic saddles. Since numerical simulations of this system need to resolve a neighborhood of the invariant subspaces very clearly, we use logarithmic coordinates [4]. The time series in Fig. 1 is for parameters that produce attracting cycling chaos; Model II produces similar behavior at this parameter value.

Suppose that cycling chaos loses stability on decreasing γ through a critical value γ_c . We can compute γ_c analytically, either from a resonance condition of Lyapunov exponents, or as follows. Suppose that a switch has just occurred and the growing variable is z , so $z \ll 1$, x is $O(1)$ and y is decaying. The evolution of z is governed by $z_{n+1} = rz_n(1-z_n)e^{-\gamma y_n}$, and this can be approximated by $z \rightarrow rz$. Starting at a switch at $z = z_0$, suppose that the number of iterations until the next switch is N . Then $z_N \approx r^N z_0$, and since z_N is $O(1)$ at a switch, $N \approx -\ln z_0 / \ln r$. While z is growing, y is decaying, and for critical γ we require $y_N = z_0$. We approximate y_N in a similar way, with y_0 an $O(1)$ number. Throughout the decay phase $y \ll 1$ but it is forced by the active variable x . Here we approximate by $y \rightarrow rye^{-\gamma x}$, and replace x by its long-term average $A_\infty [= \lim_{m \rightarrow \infty} (1/m) \sum_{i=0}^{m-1} f^i(x_0)]$ for each of the N iterations, giving $y_N \approx r^N e^{-\gamma N A_\infty}$. Then substituting our expression for N , we have $\ln y_N \approx -\ln z_0 + (\gamma \ln z_0 A_\infty) / (\ln r)$. The critical value of γ occurs when $y_N = z_0$, giving $\gamma_c = 2 \ln r / A_\infty$. The average A_∞ is easy to compute numerically, and so we obtain a curve of critical γ shown in Fig. 2. The critical γ for Model II can be found as for Model I because the dynamics in the invariant subspace $y = z = 0$ and its linearization about that subspace is identical to Model I.

One of the questions raised in Ref. [4] is what sort of attractors branch from cycling chaos at resonance. In that paper, numerical evidence was presented suggesting that the cycling chaos gives way to families of long-period periodic orbits made up of repeated segments of a single chaotic trajectory. In Model I this does not occur; for $\gamma < \gamma_c$ we find irregular cycling in which the number of iterations between switches behaves erratically. Model II, like Model I, exhibits attracting cycling above the resonance value γ_c . However,

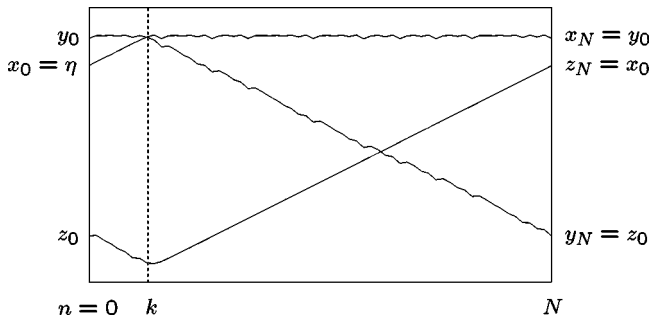


FIG. 3. Schematic diagram of a periodic orbit of period $3N$ for Model II; one third of a period is shown. This is a periodic orbit as the final and initial phases match up as shown. The iterate k shows where the phases switch.

for $\gamma < \gamma_c$ we find existence of many periodic orbits, consisting of cycles between either periodic points or chaotic trajectories (depending on the value of r). We argue that this multistability of long-period orbits is caused by, and is typical for, cycling with phase-resetting approach to chaotic saddles.

For the remainder of this note, we investigate these periodic orbits by carefully considering the evolution of the variables over one third of a periodic orbit as shown in Fig. 3. (Throughout, the period of the orbit will be $3N$.) We assume that x has just reset to $x_n = \eta$ at $n=0$, so that y is the active variable and z is in the decay phase. For a periodic orbit of period $3N$ to be possible, we require that $z_N = \eta$ —i.e., that $z_{N-1} \in [\epsilon, f(\epsilon)]$. We take $y_k = \alpha$, where α is either some $O(1)$ number \bar{A} (for a rough estimate), or more precisely takes the value $f^{N+k}(\eta)$ [since $y_0 = x_N \approx f^N(\eta)$]. There follow N iterates of forced decay. We approximate this by $y_{N+k} = r^N y_k e^{-\gamma N \beta}$, where β approximates the suppressing effect of the forcing. Again, for a rough estimate, we take β to be the long-term average A_∞ , but for a more accurate estimate we take β to be the N average $A_N = 1/N \sum_{i=0}^{N-1} f^i[f^k(\eta)]$. Since this is a periodic orbit, $y_{N+k} = z_k = r^N \alpha e^{-\gamma N \beta}$. Finally we have $(N-k-1)$ iterations of growth, approximated by $z \rightarrow rz$. This gives $z_{N-1} = r^{2N-k-1} \alpha e^{-\gamma N \beta}$. Taking logarithms, this estimate predicts that a periodic orbit will exist when

$$\ln \epsilon < (2N - k - 1) \ln r + \ln \alpha - \gamma N \beta < \ln \epsilon + \ln r,$$

that is, for the rough estimate $\alpha = \bar{A}$, $\beta = A_\infty$, for

$$N \in [N_1, N_2] = \left[\frac{a}{2 \ln r - \gamma A_\infty}, \frac{a + \ln r}{2 \ln r - \gamma A_\infty} \right],$$

where $a = \ln \epsilon - \ln \bar{A} + (k+1) \ln r$. This defines a pair of hyperbolas between which N must lie for a periodic orbit to exist, and suggests that all $N \in [N_1, N_2]$ should be present. Both ϵ and r are fixed, and k (the number of iterations from the resetting point to the next switch) can be calculated. To estimate the latter, we consider the number of iterations to take $x_0 = \eta$ to $x_k > \ln r / \gamma$ under the approximation $x_{n+1} = r x_n$ giving $k \approx [\ln(\ln r / \gamma \eta)] / \ln r$. In other words, the hyperbolas are governed by a single fitting parameter \bar{A} . Note that the de-

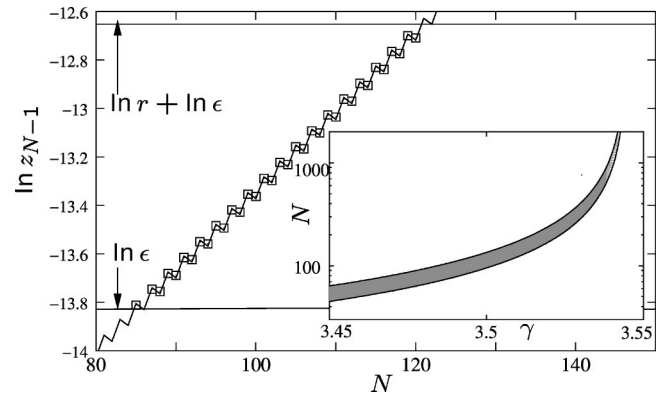


FIG. 4. Predicted and actual period $3N$ orbits for $r=3.1$, $\gamma=3.495$ for Model II. The squares indicate the location of periodic orbits, the line is the improved approximation of z_{N-1} : if it lies in the band $[\epsilon, r\epsilon]$ we predict that the resetting will lead to a stable periodic orbit. The inset shows the hyperbolas (plotted as lines) predicted by the rough estimate, with actual periodic orbits (plotted as points) lying between them ($\bar{A}=2.8$).

nomators in these expressions equal zero when $\gamma = 2 \ln r / A_\infty = \gamma_c$. Such a pair of hyperbolas can be seen in the inset of Fig. 4.

This estimate works well for the case in which the active phase of the maps is a period one point—i.e., for $r < 3$. Numerically located periodic orbits lie within the predicted hyperbolas. In particular, for a given γ we obtain all periods for N between N_1 and N_2 with a suitable choice of \bar{A} . For more complicated behavior within the invariant subspaces this estimate works less well. As r is increased the logistic map undergoes period doubling. For values of r in this region the numerically located periodic orbits still lie roughly between the predicted hyperbolas. However, we no longer find all periods for N in $[N_1, N_2]$: some are not present near N_1 and N_2 .

As r increases further, the saddles become chaotic and the bifurcation diagram of periodic orbits gets more complicated. In this case we use the improved estimate with $\alpha = f^{N+k}(\eta)$, $\beta = A_N$. This gives the estimate

$$z_{N-1} = r^{2N-k-1} f^{N+k}(\eta) e^{-\gamma N A_N}. \quad (1)$$

For fixed r , γ , ϵ , and η , z_{N-1} is a function only of N and there are no free parameters. Figure 4 plots this estimate of $\ln z_{N-1}$ for different N for $r=3.1$, and shows how it successfully predicts periodic orbits when the line falls within the band defined by $[\ln \epsilon, \ln \epsilon + \ln r]$. The squares on the diagram represent actual periodic orbits. The inset shows the hyperbolas from the simple approximation.

For values of r that give chaotic dynamics within invariant subspaces, the situation is more complicated, but the improved approximation still does a good job of predicting periodic orbits. The approximation for z_{N-1} is plotted in Fig. 5 for $r=3.75$ and $\gamma=4.01$. Figure 6 is a bifurcation diagram of periodic orbits present for the chaotic case $r=3.75$, together with the predicted envelope. The actual periodic orbits fit well inside the prediction, with the exception of some longer-

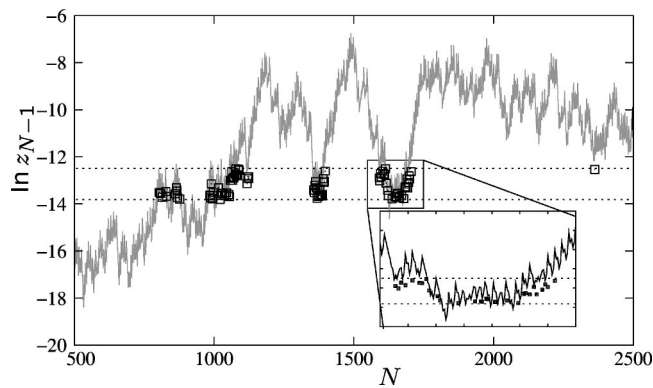


FIG. 5. Predicted and actual periodic orbits for $r=3.75$, $\gamma=4.01$ for Model II. As in Fig. 4, squares represent stable periodic orbits and the line is the approximation of z_{N-1} .

period orbits lying above the envelope. These tend to be orbits that just fail to join up and make a period $3N$ orbit, but instead become periodic after $6N$ iterations. Using this method to create an envelope not only gives a good way to predict the location of periodic orbits, but again makes clear that upon approaching γ_c we expect to find periodic orbits of increasing period. For $\gamma=\gamma_c$ the chaotic curve of $\ln z_{N-1}$ against N neither increases nor decreases on average (cf. Fig. 5), but the fluctuations, driven by the NA_N term in Eq. (1), can be expected to increase. Hence we expect periodic orbits of arbitrarily high period as the curve repeatedly crosses the band $[\epsilon, r\epsilon]$. For γ close to γ_c (above or below) the fluctuations for N large lead to possible long-periodic orbits, but eventually the linear average behavior leads the curve away from the band.

In the phase-resetting case (Model II), the qualitative dynamics is independent of the value of η . The presence of the multiplicity of periodic orbits presents an intriguing parallel between this model and the persistent phenomenon of “Newhouse sinks” in a neighborhood of a homoclinic tangency [6]. One difference is that even in the simpler case of robust cycling between periodic points in Model II, the tangency between unstable and stable manifolds will be degenerate owing to the invariant manifolds containing the con-

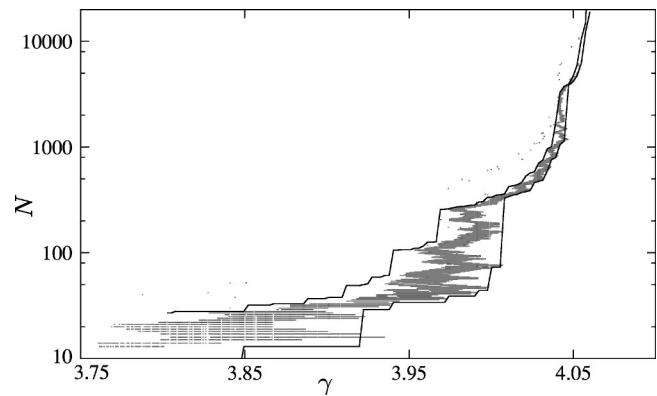


FIG. 6. Period $3N$ stable periodic orbits for Model II with $r=3.75$ are marked by dots. The lines show the predicted envelope on varying the parameter γ . The period of the periodic orbits approaches infinity as γ approaches $\gamma_c=4.061167$.

nections. Another difference is that the stable periodic orbits in this case are easy to locate numerically and indeed there appear to be no other attractors nearby. The mechanism that creates the periodic orbits in Model II resembles that found by Chawanya [7] near a robust heteroclinic network containing connections to a heteroclinic cycle. Model II is artificial in that it has a discontinuity at the phase resetting step. This means that the periodic orbits typically bifurcate from this discontinuity in a degenerate way. However, one can clearly remove this problem by smoothing out the discontinuity.

In summary, we have demonstrated how the absence (Model I) or presence (Model II) of phase resetting in the connections between saddles of a cycling (robust heteroclinic) attractor can cause qualitatively different behaviors at loss of stability of the attractor by resonance of Lyapunov exponents, even though the behaviors for attraction are similar. These models are instructive in that they are simple enough to allow a precise estimation of the location of periodic orbits while having what we believe are the main features of robust types of dynamical behavior in flows.

The research of P.A., A.R., and R.S. is supported by EPSRC Grant No. GR/N14408.

- [1] A.S. Pikovsky and P. Grassberger, *J. Phys. A* **24**, 19 (1991); H. Fujisaka and T. Yamada, *Prog. Theor. Phys.* **69**, 32 (1983); E. Ott and J.C. Sommerer, *Phys. Lett. A* **188**, 39 (1994); J.C. Alexander, I. Kan, J.A. Yorke, and Z. You, *Int. J. Bifurcation Chaos Appl. Sci. Eng.* **2**, 795 (1992); P. Ashwin, J. Buescu, and I. Stewart, *Phys. Lett. A* **193**, 126 (1994); K. Kaneko, *Phys. Rev. Lett.* **78**, 2736 (1997); S.C. Venkataramani, B.R. Hunt, E. Ott, D.J. Gauthier, and J.C. Bienfang, *ibid.* **77**, 5361 (1996).
- [2] M. Krupa, *J. Nonlinear Sci.* **7**, 129 (1997); A.S. Kuznetsov and J. Kurths (unpublished).

- [3] M. Dellnitz, M. Field, M. Golubitsky, A. Hohmann, and J. Ma, *IEEE Trans. Circuits Syst., I: Fundam. Theory Appl.* **42**, 821 (1995).
- [4] P. Ashwin and A.M. Rucklidge, *Physica D* **122**, 134 (1998).
- [5] P. Ashwin, *Chaos* **7**, 207 (1997).
- [6] J. Palis and F. Takens, *Hyperbolicity and Sensitive Chaotic Dynamics at Homoclinic Bifurcations* (CUP, Cambridge, 1995).
- [7] T. Chawanya, *Physica D* **109**, 201 (1997).